In Vivo MRI Tracking of Polyethylenimine-Wrapped Superparamagnetic Iron Oxide Nanoparticle–Labeled BMSCs for Cartilage Repair: A Minipig Model

Jiarong Chen[1], Fuyou Wang[1], Yi Zhang[1], Xuhong Jin[2],
Lin Zhang[3], Yong Feng[1], and Liu Yang[1]

Abstract

Objective: To evaluate the feasibility of tracking polyethylenimine (PEI)-wrapped superparamagnetic iron oxide (SPIO) nanoparticle–labeled, bone marrow–derived mesenchymal stem cells (BMSCs) by *in vivo* magnetic resonance imaging (MRI) in articular cartilage repair in a minipig model. *Methods:* Eighteen Guizhou minipigs were randomly divided into three groups (groups A, B, and C). In group A, PEI-wrapped SPIO nanoparticle (PEI/SPIO) and green fluorescent protein (GFP) colabeled, autologous BMSCs seeded in type II collagen gel were transplanted into the articular cartilage defects of the minipig model. In group B, GFP-labeled, autologous BMSCs seeded in type II collagen gel were transplanted. In group C, no treatment was applied for cartilage defects. All minipigs underwent clinical 3.0-T MR imaging at 4, 8, 12, and 24 weeks postsurgery. The findings were compared histologically. *Results:* Prussian staining and transmission electron microscope showed that BMSCs were efficiently labeled by PEI/SPIO. Cell viability, proliferation, and differentiation were comparable between labeled and unlabeled cells. MRI SET2WI sequence revealed that marked hypointense signal void areas representing the transplanted labeled BMSCs could be observed for at least 24 weeks. Histochemical staining confirmed the presence of Prussian blue–positive cells and GFP-positive cells at the hypointense signal void areas. At 24 weeks postsurgery, both MR signals and histologic staining of minipigs in groups A and B at the cartilage defect were close to the normal cartilage. *Conclusions:* 3.0-T MRI *in vivo* tracking of PEI/SPIO-labeled BMSCs seeded in type II collagen gel on cartilage repair following transplantation is feasible in minipigs.

Introduction

Clinically, articular cartilage defects occur commonly caused by different pathological conditions such as trauma, osteoarthritis, and rheumatoid arthritis.[1] Although there are several treatment options for cartilage defects, no one option has been established as the gold standard procedure shown to be superior to the others.[2] Tissue engineering procedures hold promise for the repair of articular cartilage defects to achieve the regeneration to hyaline cartilage. At present, numerous studies have demonstrated that bone marrow mesenchymal stem cells (BMSCs) are suitable as seed cells because they are multipotent and can differentiate into osteocytes, chondrocytes, and adipocytes lineages.[3,4] But for clinical applications, tissue engineering cell therapy is still far from satisfactory. There are many reasons behind this, one of which is that the *in vivo* behaviors of delivered stem cells are still poorly understood.[5,6] The clinical development of stem cell therapies calls for suitable methods that can follow the fate of delivered cells noninvasively *in vivo* at high resolution.[6] Magnetic resonance imaging (MRI) is

[1]Center of Joint Surgery, Southwest Hospital, The Third Military Medical University, Chongqing, China
[2]Department of Orthopedics, Haikou Hospital, Xiangya Medical College, Central South University, Hainan, China
[3]Department of Radiology, Southwest Hospital, The Third Military Medical University, Chongqing, China

Corresponding Author:
Liu Yang, The Center for Joint Surgery, Southwest Hospital of the Third Military Medical University, Chongqing 400038, China
Email: jointsurgery14@163.com

valuable to visually monitor the *in vivo* dynamic biodistribution of implanted cells by using superparamagnetic iron oxide nanoparticles for magnetic labeling of cells.[7-10] We have previously shown that clinic 1.5-T MRI could monitor the distribution and migration of the magnetically labeled rabbit MSCs in a joint cavity.[11] However, further study is needed regarding the following problems: whether there is another MRI probe with a longer tracking time for cartilage repair, whether labeled cells can be tracked when implanted into a cartilage defect similar to intra-articular injection of cells, and how to solve false positives caused by free iron.

Therefore, we tested polyethylenimine-wrapped superparamagnetic iron oxide nanoparticle (PEI/SPIO) as a label for *in vivo* monitoring of porcine BMSCs and investigated the influence of this technique on the biological properties of the cells. Then, to determine the fate of autologous BMSCs *in vivo*, we evaluated these cells labeled with SPIO and green fluorescent protein (GFP) following implantation into porcine articular cartilage defects by MR imaging using a conventional 3.0-T clinical system for 24 weeks.

Methods

Experimental Design

All studies involving animals were approved by the institute's animal care and use committee. Eighteen 12-month-old Guizhou minipigs were randomly divided into three groups (groups A, B, and C). In group A (experimental group, $n = 6$), SPIO and GFP colabeled, autologous BMSCs seeded in type II collagen gel were transplanted into the articular cartilage defects of the minipig model. In group B (negative control group, $n = 6$), GFP-labeled, autologous BMSCs seeded in type II collagen gel were transplanted. In group C (blank control group, $n = 6$), no treatment was applied to the minipigs for cartilage defects. Autologous BMSCs were harvested 3 to 5 weeks before transplantation surgery. All animals underwent clinical 3.0-T MR imaging at 4, 8, 12, and 24 weeks postsurgery. MR imaging findings were compared histologically at 24 weeks.

Cell Culture

Bone marrow was collected from the iliac crest of the minipig into a test tube containing 500 units of heparin. Monocytes layer was obtained by density centrifugation and then washed twice with phosphate-buffered saline (PBS). The cells were resuspended in DMEM (Gibco, Karlsruhe, Germany) containing 10% fetal bovine serum. Then the cells were plated into 37.5-cm² flasks.

GFP Labeling of Cells

On day 14, the cells were harvested by incubation with 0.25% trypsin and reseeded in a six-well plate at 1×10^4 cells/cm². When the cells reached 80% to 90% confluence, they were used for labeling with GFP. The primary BMSCs in a six-well plate were exposed to viral supernatant containing the lentiviral vector-mediated GFP gene (lentiviral vector, Sunbio Medical Biotechnology Co., Shang Hai, China) at a multiplicity of infection of 200 for 24 hours.[12] Subsequently, the viral supernatant was replaced with fresh medium. After having been incubated for another 48 hours, infected BMSCs, which were named GFP-BMSCs, were selected by flow cytometry. Then the GFP-BMSCs were proliferated to third passage for further use.

Iron Labeling of GFP-BMSCs and Efficiency Analysis

PEI/SPIO nanoparticles were donated by professor Ai Hua (National Engineering Research Center for Biomaterials, Sichuan University, Chengdu, China). As described previously,[13] 1.3275 g Fe/ml ferric oxide nanocomposites, positively charged with a mean zeta potential around 50 mV, with a mean hydrodynamic diameter of 79 ± 28 nm, were synthesized. The third passage of GFP-BMSCs (1×10^5 cells) were incubated with different concentrations of SPIO nanocomposites (equivalent of 4, 6, 8, 10, or 12 μg Fe/ml) for different incubation periods (6, 12, 18, 24, or 36 hours) at 37 °C in an atmosphere containing 5% CO_2.

At the end of the incubation period, the cell labeling efficiency was analyzed through Prussian blue staining and iron content measurement. For Prussian blue staining of intracellular iron particles, the cells were washed three times with PBS to remove excess SPIO. Then they were trypsinized and adhered to the slides for 24 hours, fixed with 4% glutaraldehyde, washed, incubated for 30 minutes with 2% potassium ferrocyanide in 6% hydrochloric acid, and then counterstained with nuclear fast red. Cells were considered positive on Prussian blue staining if intracytoplasmic blue granules were detected. The percentage of labeled cells was calculated with the mean of cell numbers in 10 high-power fields. The iron content was quantitatively determined by the colorimetric ferrozine assay.[14] Briefly, cells were harvested and mixed with the iron-releasing reagent. These mixtures were incubated for 2 hours at 60 °C in a fume hood. After the mixture had cooled to room temperature, the iron-detection reagent was added to each sample. Thirty minutes later, the absorbance of the sample solution was measured at 570 nm on a microplate reader. The iron content of the sample was calculated by comparing its absorbance to that of a range of standard concentrations of equal volume for three times.

Transmission Electron Microscopy Study

After SPIO probe labeling, cells were harvested, washed three times with PBS, and centrifuged (1,000 rpm, 15 minutes). The pellet was fixed in 2.5% buffered glutaraldehyde

for 30 minutes at 4 °C, followed by treatment with 1% osmium tetroxide for 30 minutes. The cells were dehydrated in a concentration gradient of ethanol, immersed in propylene-oxide, and embedded with Epon 812 (Shell Chemical Co, Houston, TX). The samples were sliced into ultrathin sections (60 nm). These sections were examined under a Tecnai-10 transmission electron microscope (Philips, Amsterdam, Netherlands).

In Vitro *BMSCs Proliferation and Differentiation Assays*

The viability of labeled BMSCs was assessed by *in vitro* proliferation assays. Briefly, labeled BMSCs were seeded into a 96-well plate (5,000 cells/well) and cell growth curves were plotted. The samples were assayed at each time point over 7 days. The absorbance at 490 nm (with 570 nm as reference wavelength) was measured by a Thermomax microplate reader (Molecular Devices, Menlo Park, CA).

Both labeled and unlabeled BMSCs were subjected to adipogenic, osteogenic, and chondrogenic differentiation to assess their differentiation capacity. The cells were maintained in six-well plates for 21 days in the presence of differentiation supplements as described elsewhere. Adipogenic cells were stained with oil red-O (Sigma, St Louis, MO), and chondrogenic cells with Toluidine blue (Sigma) to display glycosaminoglycan. Type II collagen production was assessed by standard immunohistochemistry using anti-collagen II antibody (mouse anti-rabbit IgG, Biochemicals, Costa Mesa, CA). Osteogenic cells were stained with alizarin red to reveal calcium deposition.

In Vitro *Cellular MRI*

To determine the sensitivity of the MRI magnets for the detection of labeled cells, labeled BMSCs labeled with different concentrations of SPIO nanocomposites (equivalent of 4, 6, 8, 10, or 12 μg Fe/ml) were trypsinized, centrifuged, and resuspended in 0.5 ml of 1% agarose (5×10^3, 1×10^4, 5×10^4, 1×10^5, 5×10^5, 1×10^6, 5×10^6 labeled cells). Then the tubes were placed into a box filled with water. *In vitro* cellular imaging was performed on a clinical 3.0-T MR imager (GE company Singa EXCITE HDx) using a T2-weighted spin-echo (SET2WI) sequence. Sequence parameters were as follows: repetition time = 4000 ms, echo time = 90 ms, flip angle = 120°, field of view = 220 × 171 mm, matrix size = 240 × 384, slice thickness = 2 mm, slice gap = 0 mm.

Transplantation of Double-Labeled BMSCs

All Guizhou minipigs were anesthetized with intravenous pentobarbital sodium (0.03 g/kg). The hind legs were shaved and draped in a sterile fashion. According to the methods described by Mierisch *et al.*,[15] an anteromedial skin incision was made at the knee to expose the articular surface of the femur through a small medial parapatellar arthrotomy. A trochlear cartilage defect, 6 mm in diameter and 3 mm in depth, was then created in the trochlear groove of knee by drilling with an air-powered Keith needle. Then SPIO and GFP double-labeled (group A) or unlabeled (group B) BMSCs (5×10^7) seeded in 1 ml of type II collagen gel (supported by Laboratory of Joint Surgery, Southwest Hospital, Chongqing, China) were transplanted into the cartilage defect. The collagen type II hydrogel used in this study is a natural polymer derived from pig's joint cartilages, which becomes a gel through physical crosslinking when the temperature rises to 37 °C. This polymer was demonstrated to have good cell compatibility, and it is currently going through a patent application process. After being heated by incandescent light for 5 minutes, the incision was closed in layers routinely. After surgery, all the animals were allowed to move freely in their pig sty.

In Vivo *MR Imaging*

The minipigs were imaged under general anesthesia at 4, 8, 12, and 24 weeks postsurgery, and MR images of the porcine joints were obtained on a clinical 3.0-T MR imager equipped with knee coil. Sagittal and axial images were obtained by a SET2WI sequence. Imaging parameters were as follows: repetition time = 4000 ms, echo time = 90 ms, flip angle = 120°, field of view = 220 × 171 mm, matrix size = 240 × 384, slice thickness = 2 mm, slice gap = 0 mm.

Histology

The minipigs were sacrificed at 24 weeks after surgery. Macroscopic observations on the defect sites and surrounding joint tissues were made at necropsy. For histological evaluations, the synovium at the suprapatellar bursa, the popliteal space site, and bone-cartilage samples were carefully dissected and fixed in 4% formaldehyde solution for 5 to 7 days, then decalcified in 8% EDTA solution for as long as 3 weeks, and embedded in paraffin in 5-mm-thick sections. The sections were stained with hematoxylin and eosin before histological examination.

Transplanted BMSCs were detected by Prussian blue staining and anti-GFP staining using a FITC-conjugated goat anti-mouse IgG (Cappel, Durham, NC) as a secondary antibody. To estimate hyaline cartilage formation in the repair tissue, safranin-O staining was used to evaluate the glycosaminoglycan content. It was assumed that tissue that was stained pink or red by safranin O was cartilage.

Statistical Analysis

Statistical analysis was performed using two-tailed unpaired *t*-test and one-way ANOVA followed by Tukey's multiple comparison test using SPSS software (SPSS v12.0; IBM

SPSS, Cary, NC). If we found statistical differences between periods, we used Fisher's PLSD tests for post hoc multiple comparisons. In the data collection, the experimenters were blind to the group identities. A *P* value of <0.05 was considered significant.

Results

GFP Labeling of Cells

GFP expression was observed 24 hours after transfection. Three days later, the GFP expression rate was 85 ± 5%. Under inverted fluorescence microscopy, significant GFP expression was observed in the cell nuclei and cytoplasm. The cells were fusiform in morphology.

Iron Labeling of GFP-BMSCs

GFP-BMSCs can be directly labeled with SPIO nanocomposites by adding probes to the culture medium after 24-hour incubation, with the final iron concentration ranging from 4 to 12 μg/ml. It is evident that nearly 100% of the GFP-BMSCs were labeled at concentrations of 8, 10, and 12 μg/ml by Prussian blue staining (8 μg/ml: 95.5 ± 2.5%, 10 μg/ml: 97.2 ± 2.8%, 12 μg/ml: 100%), which was significantly higher than at concentrations of 4 and 6 μg/ml (4 μg/ml: 50.5 ± 5.4%, 6 μg/ml: 70.2 ± 1.8%) (**Fig. 1A-E**). There was no obvious morphological change between the labeled cells at concentrations of 4, 6, and 8 μg/ml and unlabeled cells. However, treatment with 10 and 12 μg/ml for 24 hours impaired cell survival and proliferation significantly. Cell labeling was further confirmed by transmission electron microscopy, which revealed SPIO probes confined in the intracellular space (**Fig. 1F**, arrows pointed) but not in cell nuclei. The colorimetric ferrozine assay showed the SPIO uptake process in BMSCs was a time- and dose-dependent behavior (**Fig. 1G**). Longer incubation time or higher incubation iron concentration or both led to higher cellular iron content. Cells labeled with 4 μg Fe/ml for 24 hours have similar iron content as 12 μg Fe/ml for only 6 hours ($P > 0.05$). However, the iron content of 36 hours labeling at 10 and 12 μg Fe/ml was lower than 24 hours labeling. On the basis of these results, we decided to use SPIO at 8 μg Fe/ml for a 24-hour incubation time.

In Vitro *MSC Proliferation and Differentiation Assays*

MTT cytotoxicity and proliferation assay demonstrated no significant decreases of proliferation of SPIO-labeled cells compared with that of unlabeled cells over 7 days ($P > 0.05$) (**Fig. 2**). *In vitro* cell differentiation analysis indicated that cell differentiation and morphology were similar between labeled and unlabeled BMSCs.

In Vitro *Cellular MRI*

SE T2WI images revealed the presence of a hypointense signal (**Fig. 3**). A good linear correlation among the number of labeled cells, concentrations of SPIO, and optical density of the MR imaging was observed by SI loss analysis. The numbers of hypointense regions increased with increasing concentrations of labeled BMSCs or number of labeled cells.

### In Vivo *MR Tracking of BMSCs*

At 4 weeks postoperation of transplanting SPIO/GFP colabeled autologous BMSCs to cartilage defect, marked hypointense signal void areas representing the transplanted BMSCs could be observed in cartilage defect of group A on SET2WI MR images. At 8 weeks postoperation, signal changes could also be distinguished visually between the defect and the normal cartilages. At 12 weeks postoperation, recognizable hypointense artifacts caused by iron-positive cells in the defects were detected, although it became lower than that in 4 weeks. At 24 weeks postoperation, MRI SET2WI sequence revealed marked hypointense signal void areas representing the transplanted BMSCs (**Fig. 4**). No contrast can be observed on MR images of unlabeled cells and controls.

Histological Evaluation of 6-Month Repair Tissues

At the time of necropsy at 24 weeks, safety tests indicated that the treatment of defects with BMSCs seeded in type II collagen did not give rise to any lasting lameness, effusion, or systemic inflammation. After 24 weeks of repair, compared with the defects in group C, those in groups A and B were filled with hyaline cartilage, which was stained with safranin O for proteoglycans (**Fig. 5B** and **F**). Prussian blue stained (**Fig. 5C**) and GFP-positive cells (**Fig. 5D**) were observed in the repair tissue in group A. Cartilage defects in group C were most frequently observed to be repaired with fibrous tissue, which was negative on safranin O staining. No Prussian blue or GFP-positive cells were detected in the synovium at the suprapatellar bursa and the popliteal space site in all groups.

Discussion

In this article, we found that using 3.0-T MRI is possible to *in vivo* trace PEI/SPIO-labeled BMSCs from minipig on SET2WI sequence by the change of signal intensity for at least 24 weeks. We used type II collagen gel for cell-based construct because it is similar to the component of normal cartilage than type I that has been reported previously.[16] At present, this is the first time that PEI/SPIO and GFP
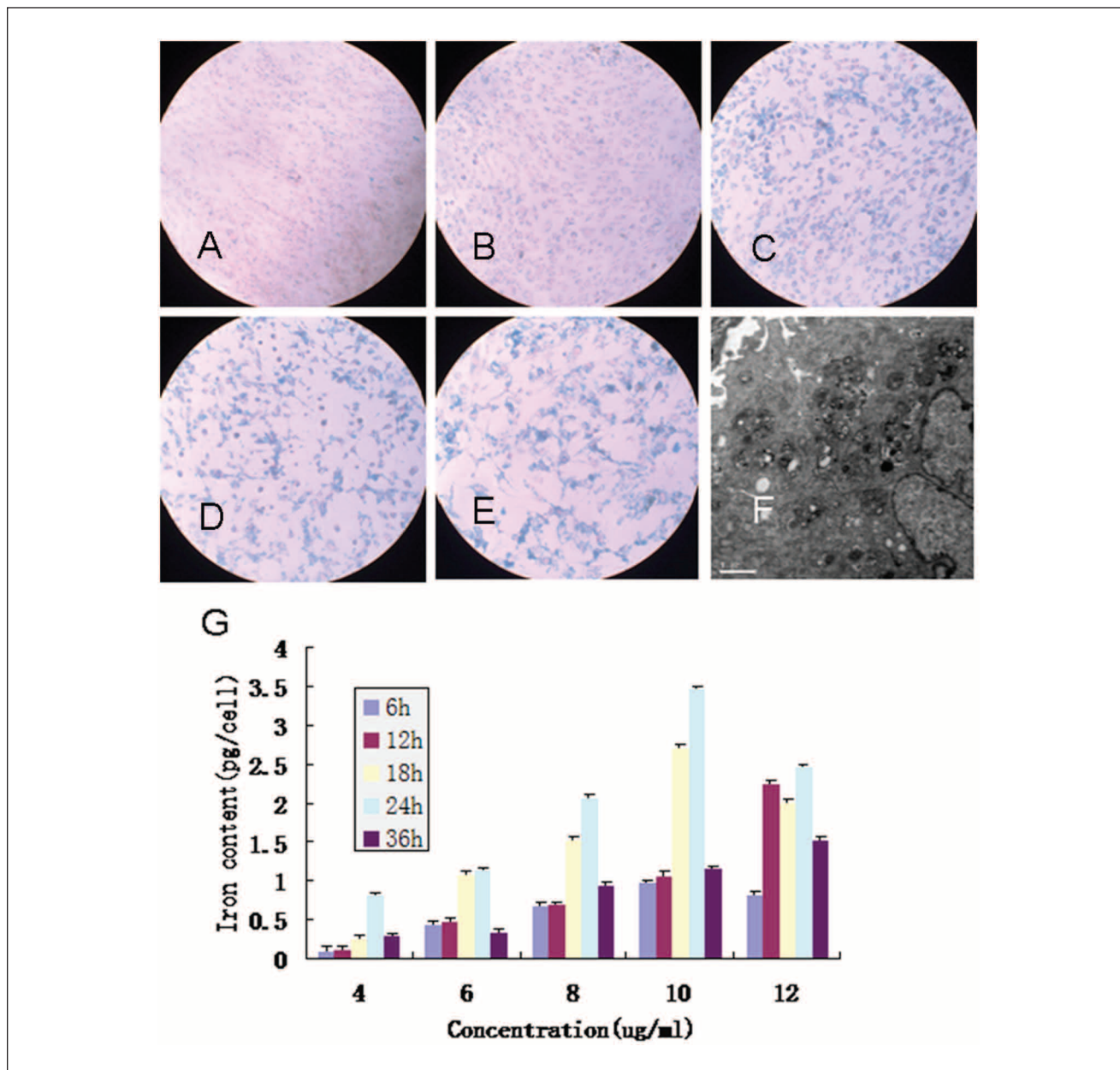
Figure 1. (**A-E**) Prussian blue staining of green fluorescent protein (GFP) bone marrow mesenchymal stem cells (BMSCs) incubated with different concentrations of polyethylenimine-wrapped superparamagnetic iron oxide (PEI/SPIO) nanocomposites. (**A**) 4 µg/ml; (**B**) 6 µg/ml; (**C**) 8 µg/ml; (**D**) 10 µg/ml; (**E**) 12 µg/ml. (**F**) Transmission electron micrographs of GFP-BMSC labeled with 8 µg/ml SPIO (10,000x). (**G**) Cellular iron content of MSCs after labeling. The iron uptake process in MSCs displays a time- and dose-dependent behavior.

double-labeled BMSCs seeded in type II collagen gel has been used for articular cartilage defects repair and *in vivo* MRI tracking.

Our *in vitro* data revealed that PEI/SPIO was a good choice for tracking BMSCs in cartilage repair. Previously, dextran-coated SPIO, such as AMI225 (feridex), AMI2227 (ferumoxtran), AMI2121 (LUMIREM), and SHU555A (resovist),[17,18] acting as the stem cell probe, has some obvious limits. First, dextran-coated SPIO particles alone cannot be internalized into the cytoplasm of nonphagocytic cells. Usually it needs to be mixed with protamine or poly-L-lysine (PLL) so that the surface charge of SPIO is changed from negative to positive.[19] Second, *in vivo* degradation time of dextran-coated SPIO is too short for cartilage repair tracking, although the longest tracing time was 12 weeks in our previous report.[7] In this study, however, we found that
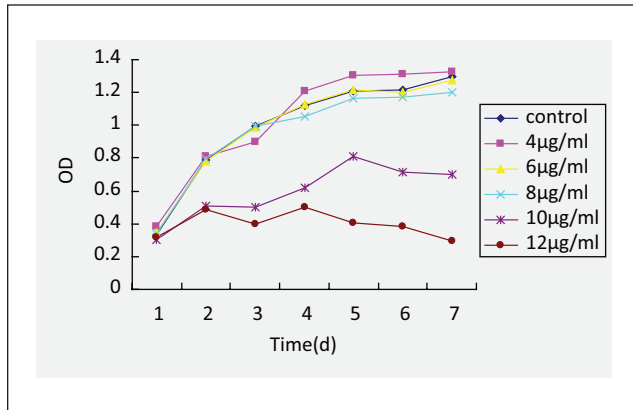
Figure 2. Growth curves of the five groups of labeled cells and the control.
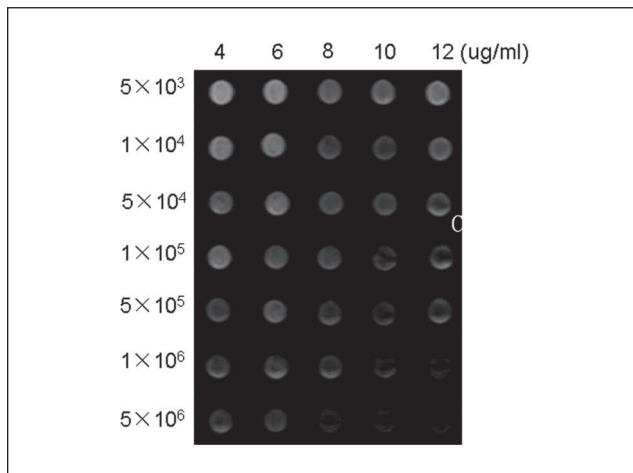
Figure 3. *In vitro* cell MRI. SET2WI of the 35 Eppendorf tubes. From right to left: 12 μg/ml, 10 μg/ml, 8 μg/ml, 6 μg/ml, 4 μg/ml of polyethylenimine-wrapped superparamagnetic iron oxide nanocomposites; from top to bottom: 5×10^3, 1×10^4, 5×10^4, 1×10^5, 5×10^5, 1×10^6, 5×10^6 labeled cells.

the PEI/SPIO had longer *in vivo* degradation time (at least 24 weeks) than the dextran-coated SPIO. However, it was easy to be internalized into BMSCs because of their positively charged surface.

More important, we established a PEI/SPIO-based protocol to label BMSCs yielding high label efficiency while preserving the functional properties of the labeled cells. Our studies showed that BMSCs can be efficiently labeled with 8 μg/ml SPIO for 24 hours. More than 99% positive rate of Prussian blue staining cells had been found. And neither survival nor proliferation potential is severely impaired in dealing with 8 μg Fe/ml for 24 hours. However, treatment with 10 or 12 μg Fe/ml for 24 hours impaired cell survival and proliferation significantly. This indicates that SPIO

concentration and incubation time should be carefully taken into account when developing preclinical strategies relying on SPIO-based cell tracking techniques. We could solve the problem by reducing both the SPIO concentration and the incubation time. Doses of 8 μg Fe/ml for 12 or 24 hours, or doses of 6 μg Fe/ml for 24 hours, results in efficient cell labeling without impairment of cell survival and proliferation potential.

For MRI detection, significant signal intensity decreases were observed with labeled BMSCs on SET2WI sequences,[20] which had the highest percentage of SI change due to its higher sensitivity to iron oxide particles, and a higher cell concentration led to a greater change in the signal intensity, indicating that there was a good correlation between the number of cells and the signal intensity. On the other hand, we found that a good linear correlation between the iron content of cells and optical density of the MR imaging in our study.

To validate if the SPIO-generated signal was related to originally labeled cells, or that SPIO particles were taken up by host cells, GFP-transfected BMSCs were colabeled with SPIO. Our study confirmed that GFP lentiviral vector and PEI/SPIO could effectively label BMSCs without impairing cell proliferation and differentiation. For the purpose of additional detection, we found that SPIO-positive cells in the cartilage defect by MR imaging while GFP could be found at these regions by histology. The rate of colabeled cells accounted to 60.5%. By doubly labeling the BMSC with GFP gene and SPIO nanoparticles, this study clearly showed that the transplanted BMSC extensively multiply during their survival in the cartilage defect. The finding that the GFP-positive cells contained SPIO nanoparticles, therefore, proves their excessive facility of proliferation in the cartilage defect. At the same time, we excluded the false positives caused by free iron.

In this present study, we established a joint cartilage defect model of a clinically relevant size (6 mm in diameter and 3 mm in depth) and provided direct evidence that SPIO-labeled BMSCs can be identified in the cartilage defect after cell transplantation and that these cells contribute to the regions of signal loss observed in MR images of knee joint. This was achieved using our minipig model in which BMSCs were GFP and SPIO-positive labeled. With this unique minipig model, we showed excellent correspondence between areas in the cartilage defect that were GFP-positive and SPIO-positive, and we showed that these areas could be related to regions of signal loss observed in MR images of knee joint.

In summary, we consider PEI/SPIO labeling at optimal low dosages that allows maintaining stable biological features without toxicity to hold great potential for clinically translatable cell tracking using MRI in cell-based cartilage repair. This would show the distribution and diffusion of
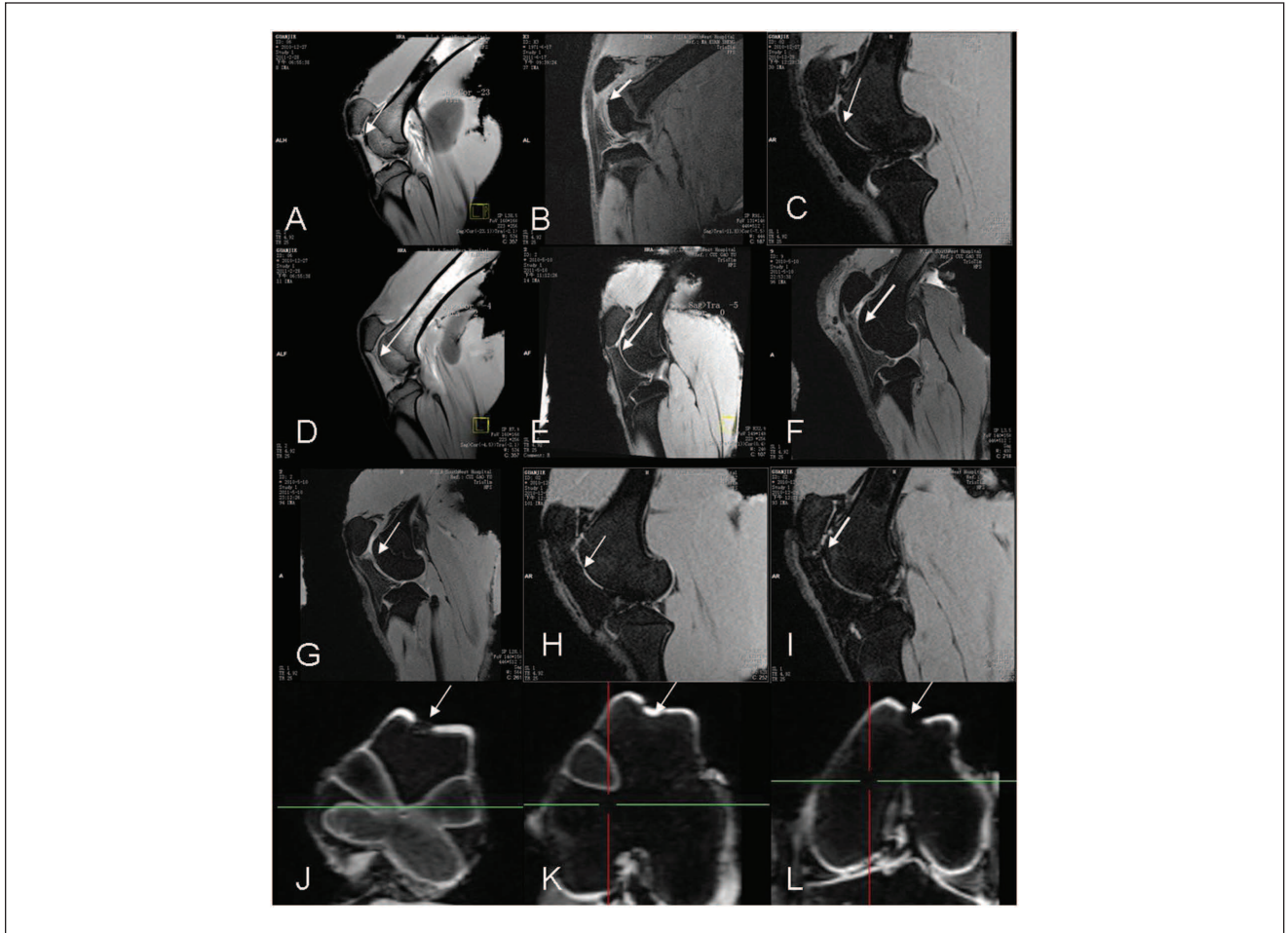
Figure 4. SET2WI multisection magnetic resonance images (4000/90; flip angle, 120°) of the knee of an experimental minipig model of articular cartilage defect at 4, 8, 12, and 24 weeks *in vivo*. (**A**, **B**, **C**, **G**) Sagittal image of group A after cell transplantation of 5×10^7 bone marrow mesenchymal stem cells (BMSCs) seeded in type II collagen gel at 4, 8, 12, and 24 weeks. Low signal intensity indicates the presence of superparamagnetic iron oxide (SPIO)-labeled BMSCs. (**D**, **E**, **F**, **H**) Sagittal image of group B after cell transplantation of 5×10^7 BMSCs seeded in type II collagen gel. (**J**, **K**) Coronal image of group A after cell transplantation of 5×10^7 BMSCs seeded in type II collagen gel at 24 weeks. (**I**, **L**) Image of group C at 24 weeks. The arrows indicate SPIO-labeled cells.
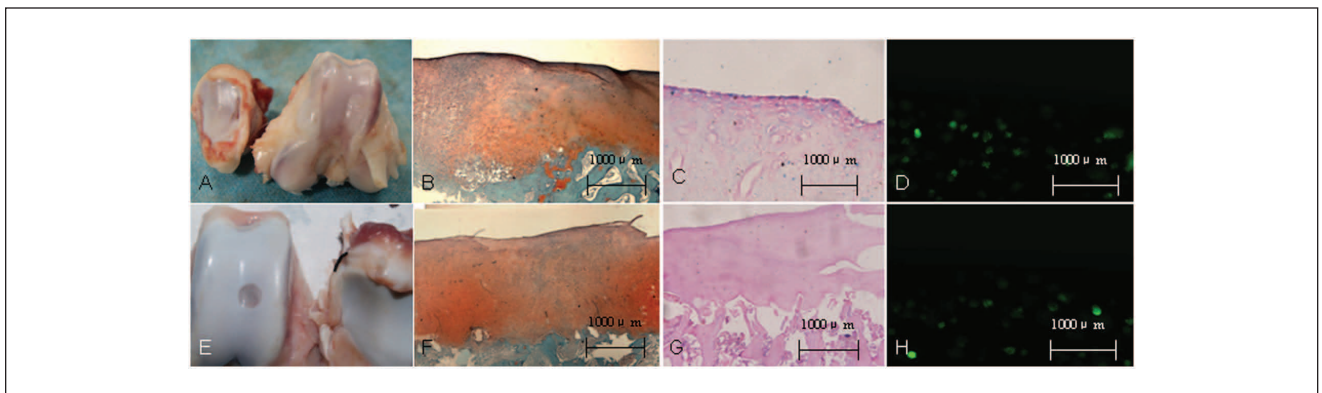
Figure 5. Gross observation and histological evaluation of cell transplantation of superparamagnetic iron oxide (SPIO)-labeled bone marrow stem cells (BMSCs) in the knee of an experimental minipig model of articular cartilage defects at 24 weeks after surgery. (**A**, **E**) Gross observation for group A and group B. (**B**, **F**) Safranin-O staining showed proteoglycan deposition in trochlear groove defects at 24 weeks after surgery. (**C**, **G**) Prussian blue staining for the defect region. (**D**, **H**) Fluorescence microscopy demonstrated green fluorescence of BMSCs labeled with green fluorescent protein at defect region.

the labeled cells, thereby elucidating the regenerative mechanisms and providing opportunities to improve current repair strategies.

Acknowledgments and Funding

Declaration of Conflicting Interests

The author(s) declared no potential conflicts of interest with respect to the research, authorship, and/or publication of this article.

References

1. Browne JE, Branch TP. Surgical alternatives for treatment of articular cartilage lesions. J Am Acad Orthop Surg. 2000;8: 180-9.

2. O'Driscoll SW. The healing and regeneration of articular cartilage. J Bone Joint Surg Am. 1998;80:1795-812.

3. Jiang Y, Jahagirdar B, Reinhardt RL, Schwartz RE, Keene CD, Ortiz-Gonzalez XR, et al. Pluripotency of mesenchymal stem cells derived from adult marrow. Nature. 2002;418:41-9.

4. Pettenger MF, Mackay AM, Beck SC, Jaiswal RK, Douglas R, Mosca JD, et al. Multilineage potential of adult human mesenchymal stem cells. Science. 1999;284:143-7.

5. Lerou PH, Daley GQ. Therapeutic potential of embryonic stem cells. Blood Rev. 2005;19:321-31.

6. Schroeder T. Imaging stem-cell-driven regeneration in mammals. Nature. 2008;453:345-51.

7. Arbab AS, Bashaw LA, Miller BR, Jordan EK, Lewis BK, Kalish H, et al. Characterization of biophysical and metabolic properties of cells labeled with superparamagnetic iron oxide nanoparticles and transfection agent for cellular MR imaging. Radiology. 2003;229:838-46.

8. Frank JA, Miller BR, Arbab AS, Zywicke HA, Jordan EK, Lewis BK, et al. Clinically applicable labeling of mammalian and stem cells by combining superparamagnetic iron oxides and transfection agents. Radiology. 2003;228:480-7.

9. Arbab AS, Bashaw LA, Miller BR, Jordan EK, Bulte JWM, Frank JA. Intracytoplasmic tagging of cells with ferumoxides and transfection agent for cellular magnetic resonance imaging after cell transplantation: methods and techniques. Transplantation. 2003;76:1123-30.

10. Bulte JW, Duncan ID, Frank JA. In vivo magnetic resonance tracking of magnetically labeled cells after transplantation. J Cereb Blood Flow Metab. 2002;22:899-907.

11. Jing XH, Yang L, Duan XJ, Xie B, Chen W, Li Z, et al. In vivo MR imaging tracking of magnetic iron oxide nanoparticle labeled, engineered, autologous bone marrow mesenchymal stem cells following intra-articular injection. Joint Bone Spine. 2008;75:432-8.

12. Duan X, Yang L, Dong S, Xin R, Chen G, Guo L. Characterization of EGFP-labeled mesenchymal stem cells and redistribution of allogeneic cells after subcutaneous implantation. Arch Orthop Trauma Surg. 2008;128:751-9.

13. Mizuno K, Muneta T, Morito T, Ichinose S, Koga H, Nimura A, et al. Exogenous synovial stem cells adhere to defect of meniscus and differentiate into cartilage cells. J Med Dent Sci. 2008;55:101-11.

14. Riemer J, Hoepken HH, Czerwinska H, Robinson SR, Dringen R. Colorimetric ferrozine-based assay for the quantitation of iron in cultured cells. Anal Biochem. 2004;331:370-5.

15. Mierisch CM, Wilson HA, Turner MA, Milbrandt TA, Berthoux L, Hammarskjold ML, et al. Chondrocyte transplantation into articular cartilage defects with use of calcium alginate: the fate of the cells. J Bone Joint Surg Am. 2003; 85-A:1757-67.

16. Heymer A, Haddad D, Weber M, Gbureck U, Jakob PM, Eulert J, et al. Iron oxide labelling of human mesenchymal stem cells in collagen hydrogels for articular cartilage repair. Biomaterials. 2008;29:1473-83.

17. Arbab AS, Liu W, Frank JA. Cellular magnetic resonance imaging: current status and future prospects. Expert Rev Med Devices. 2006;3:427-39.

18. Wang YX, Hussain SM, Krestin GP. Superparamagnetic iron oxide contrast agents: physicochemical characteristics and applications in MR imaging. Eur Radiol. 2001;11:2319-31.

19. Bulte JWM, Kraitchman DL. Monitoring cell therapy using iron oxide MR contrast agents. Curr Pharm Biotechnol. 2004;5:567-84.

20. Arbab AS, Frenkel V, Pandit SD, Anderson SA, Yocum GT, Bur M, et al. Magnetic resonance imaging and confocal microscopy studies of magnetically labeled endothelial progenitor cells trafficking to sites of tumor angiogenesis. Stem Cells. 2006;24:671-8.